MATERIALS SCIENCE

Stimulus-responsive room temperature phosphorescence materials with full-color tunability from pure organic amorphous polymers

Dan Li[1], Jie Yang[1]*, Manman Fang[1], Ben Zhong Tang[1,2]*, Zhen Li[1,3,4,5,6]*

Achieving stimulus-responsive ultralong room temperature phosphorescence (RTP) in organic materials especially with full-color tunable emissions is attractive and important but rarely reported. Here, a strategy was reported to realize stimulus-responsive RTP effect with color-tunable emissions by using water as solvent in the preparation process without any organic solvent through covalent linkage of arylboronic acids with different π conjugations and polymer matrix of polyvinyl alcohol. The yielded polymer films exhibit outstanding RTP performance (2.43 s). Furthermore, an excitation-dependent RTP film was obtained, and the afterglow color changes from blue to green, then to red as the excitation wavelength increases. The RTP property of all the above materials is sensitive to water and heat stimuli, because the rigidity of the system could be broken by water. Last, they were successfully applied in a multilevel information encryption and multicolor paper and ink.

INTRODUCTION

Stimulus-responsive luminescent materials have garnered tremendous interests in recent years because of the widespread potential application in many fields, such as information storage and anti-fake and optoelectronic devices (*1*–*9*). Compared with numerous stimulus-responsive materials based on fluorescence in previous reports (*10*–*12*), little effort has been spent on the study of the ones on room temperature phosphorescence (RTP). The much longer emission lifetime even observed by naked eye of RTP materials makes them more conducive to be monitored under external stimuli (*13*–*18*). Nevertheless, the exploration of stimulus-responsive RTP materials is still at the preliminary stage, mainly because the RTP emission tends to be realized in the crystal state, and the disadvantages of crystal including bad repeatability and poor solution processability greatly limit their applications (*19*–*20*). To overcome these drawbacks, amorphous RTP systems were explored, which usually create a rigid environment (*21*–*24*). Particularly, doping small organic molecules into rigid polymers is even more attractive on account of the film-forming ability of polymer, which is beneficial for diverse technical applications with flexibility and easy processing procedures (*25*–*30*).

In addition, the majority of stimulus-responsive RTP materials only exhibit single emission color signal, while practical applications still rely on multidimensional signals involving multicolor. Tunable emission color makes stimulus-responsive RTP materials more practical in various fields (*30*–*33*). For instance, Zhao and co-workers (*34*) reported a color-tunable organic RTP polymeric system that is sensitive to water, achieving visible and multilevel information encryption. However, the color signal is limited to the change from blue to yellow, whereas Dou *et al.* (*35*) showed a full-color tunable RTP system depending on excitation wavelength. It is a pity that it cannot respond to other external stimuli, which limits their application to a higher stage, such as multilevel information encryption and decryption. Apparently, multisignal luminescent materials have more practical application values. Hence, it is still a great challenge to achieve RTP materials that show full-color tunability in response to external stimulus, such as pH, light, humidity, temperature, and pressure.

Here, we developed a series of stimulus-responsive RTP materials with full-color tunability based on arylboronic acids and polyvinyl alcohol (PVA) via a facile dehydration condensation reaction. According to previous studies, the arylboronic acid or arylboronic acid ester could exhibit outstanding phosphorescent property in rigid environment (i.e., 77 K) or under mechanical stimulation, and the existence of boronic acid unit tends to occur dehydration condensation reaction with PVA (*36*–*38*). Inspired by these, five arylboronic acids were chosen as phosphorescent chromophores (Fig. 1A). With the expansion of π conjugation degrees of aromatic groups in arylboronic acids from biphenyl to naphthalene, then to pyrene, the corresponding photoluminescence emissions of polymer films tend to redshift, leading to satisfactory color tuning. There are two reasons for using PVA as the polymer matrix. On the one hand, PVA is a rigid polymer matrix rich in hydroxyl groups, which could react with the hydroxyl groups of arylboronic acid to form B—O covalent bonds, restricting the thermal motion of molecules to facilitate their RTP emission with long RTP lifetimes even in the amorphous state. On the other hand, the excellent hydroscopicity of PVA makes it easy to respond to humidity, changing the rigidity of PVA chains. Therefore, resultant RTP property could be easily controlled by the alternating stimulation of heat and water (fig. S1). When reacting *m*-Bp-BOH, Nap-BOH, and Py-BOH with PVA simultaneously, an excitation-dependent RTP material was obtained (Fig. 1C). At this time, the stimulus-responsive property of material could still be retained, as PVA matrix acted as the stimulus-responsive site. Moreover, the fabrication processes of these materials were

[1]Institute of Molecular Aggregation Science, Tianjin University, Tianjin 300072, China. [2]Shenzhen Institute of Molecular Aggregate Science and Engineering, School of Science and Engineering, The Chinese University of Hong Kong, Shenzhen, Guangdong 518172, China. [3]Tianjin Key Laboratory of Molecular Optoelectronic Sciences, Department of Chemistry, Tianjin University, Tianjin 300072, China. [4]Hubei Key Lab on Organic and Polymeric Optoelectronic Materials, Department of Chemistry, Wuhan University, Wuhan 430072, China. [5]Joint School of National University of Singapore and Tianjin University, International Campus of Tianjin University, Binhai New City, Fuzhou 350207, China. [6]Wuhan National Laboratory for Optoelectronics, Huazhong University of Science and Technology, Wuhan 430074, China.
*Corresponding author. Email: jieyang2018@tju.edu.cn (J.Y.); tangbenz@cuhk.edu.cn (B.Z.T.); lizhen@whu.edu.cn (Z.L.)

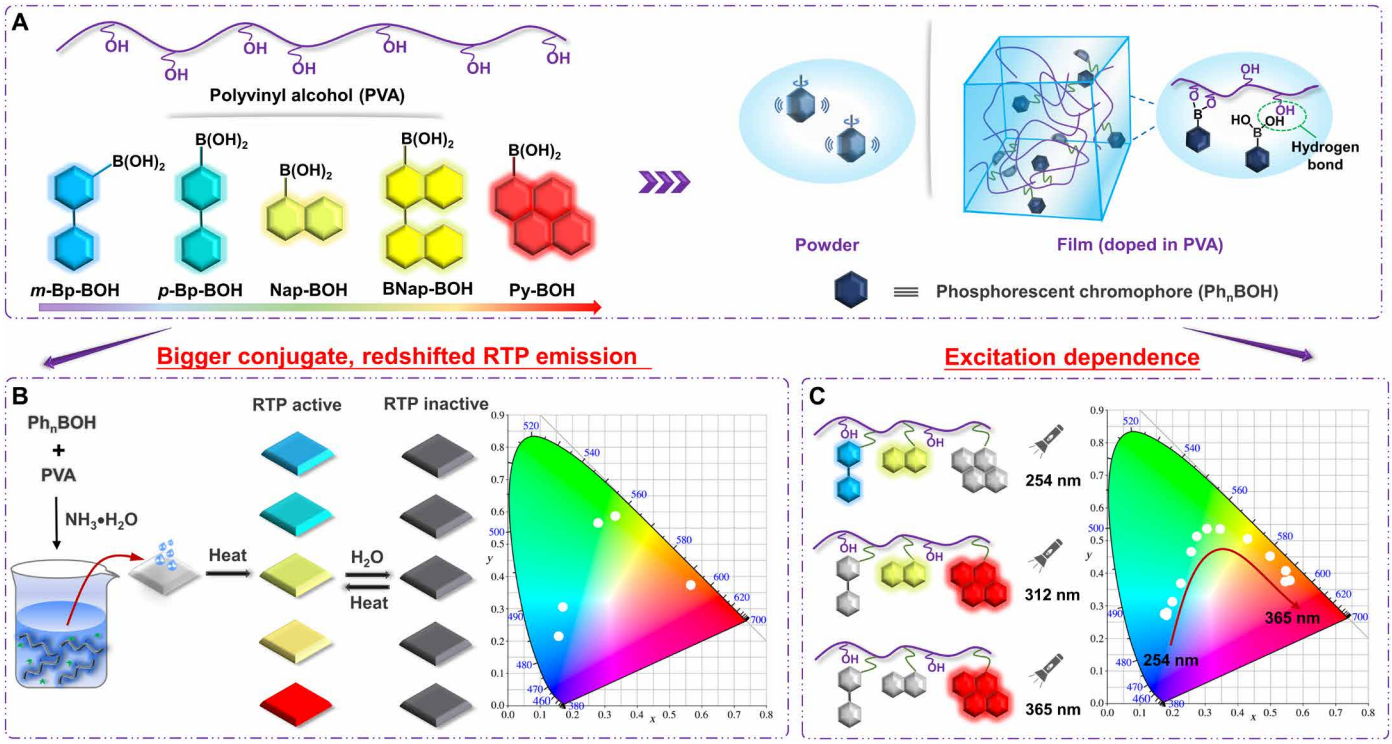

Fig. 1. Stimulus-responsive color-tunable room temperature phosphorescent system. Schematic illustration of (**A**) room temperature phosphorescence mechanism of polymer film, (**B**) the synthetic process of five target products and changes in RTP behaviors under heating or water stimulus, and (**C**) the excitation wavelength–dependent room temperature phosphorescence mechanism of polymer film.

completed in pure aqueous phase without any organic solvents, which is environmentally friendly. Besides, the low cost of raw materials, simple synthetic method, and mild synthetic conditions make them easy to be commercialized. It will provide a new perspective for designing stimulus-responsive ultralong RTP materials with color-tunable emissions.

RESULTS

Stimulus-responsive RTP property

As shown in Fig. 1B, five polymer films, namely, *m*-Bp-BOH-PVA, *p*-Bp-BOH-PVA, Nap-BOH-PVA, BNap-BOH-PVA, and Py-BOH-PVA, were prepared via a facile dehydration condensation reaction between PVA and five arylboronic acids (*m*-Bp-BOH, *p*-Bp-BOH, Nap-BOH, BNap-BOH, and Py-BOH) (mass ratio = 100:1, except for the Py-BOH, which is 100:2) upon the addition of ammonia water, an alkali containing no metal and easy to evaporate after the dry film forming. The reaction yields were proved to be 50.29, 45.96, 59.18, 46.32, and 46.52% for *m*-Bp-BOH-PVA, *p*-Bp-BOH-PVA, Nap-BOH-PVA, BNap-BOH-PVA, and Py-BOH-PVA, respectively, by ultraviolet-visible (UV-vis) absorption measurement (fig. S2). Then the photophysical properties of these five desiccative polymer films were investigated in detail (Fig. 2 and figs. S3 to S7). Because of the extended π conjugation of arylboronic acids, both the fluorescence spectra and the RTP spectra of five polymer films showed redshifted characteristics from *m*-Bp-BOH-PVA/*p*-Bp-BOH-PVA to Nap-BOH-PVA/BNap-BOH-PVA, then to Py-BOH-PVA film (Fig. 2B). Time-resolved emission decay curves show that *m*-Bp-BOH-PVA film exhibits the longest RTP lifetime, reaching up to 2.43 s, and the blue afterglow could be captured by naked eyes even lasting for 10 s when the UV lamp was turned off, surpassing most of the organic RTP materials under ambient condition (Fig. 2C) (*38*–*40*). In addition, the corresponding RTP quantum yield could achieve 5.40%. On the other hand, the Py-BOH-PVA film shows the highest RTP quantum yield of 13.10% with red emission, and the RTP lifetime can also reach 0.34 s (Fig. 2B). In addition, the excitation-dependent RTP emission could be found for Py-BOH-PVA film for the formation of aggregates to some extent (figs. S8 and S9).

To further investigate whether the water does have an effect on the RTP emission of these films, we studied their RTP behaviors after alternating stimulation of heat and water (Fig. 2B). Taking *m*-Bp-BOH-PVA film as an example, the prepared film fumed by water vapor for 10 min was measured first, which showed nearly no RTP emission at 470 nm. Then, after certifying its good thermostability (figs. S10 and S11 and table S1), the film was heated at 85°C for 10 min and dropped to room temperature, and the resultant phosphorescence emission at 470 nm enhanced a lot (Fig. 2B). By this time, the water in the film should be considered to be almost removed. Besides, excellent photostability could be observed for it (fig. S12). Subsequently, when the film was fumed by water vapor again, the RTP intensity of the 470-nm emission band decreased. Thus, the RTP property of the film could be controlled by alternant heating and water fumigation, and the cycle could be repeated at least five times (figs. S13 and S14). Likewise, the other four films all exhibited the similar properties as the *m*-Bp-BOH-PVA film (figs. S15 and S22).

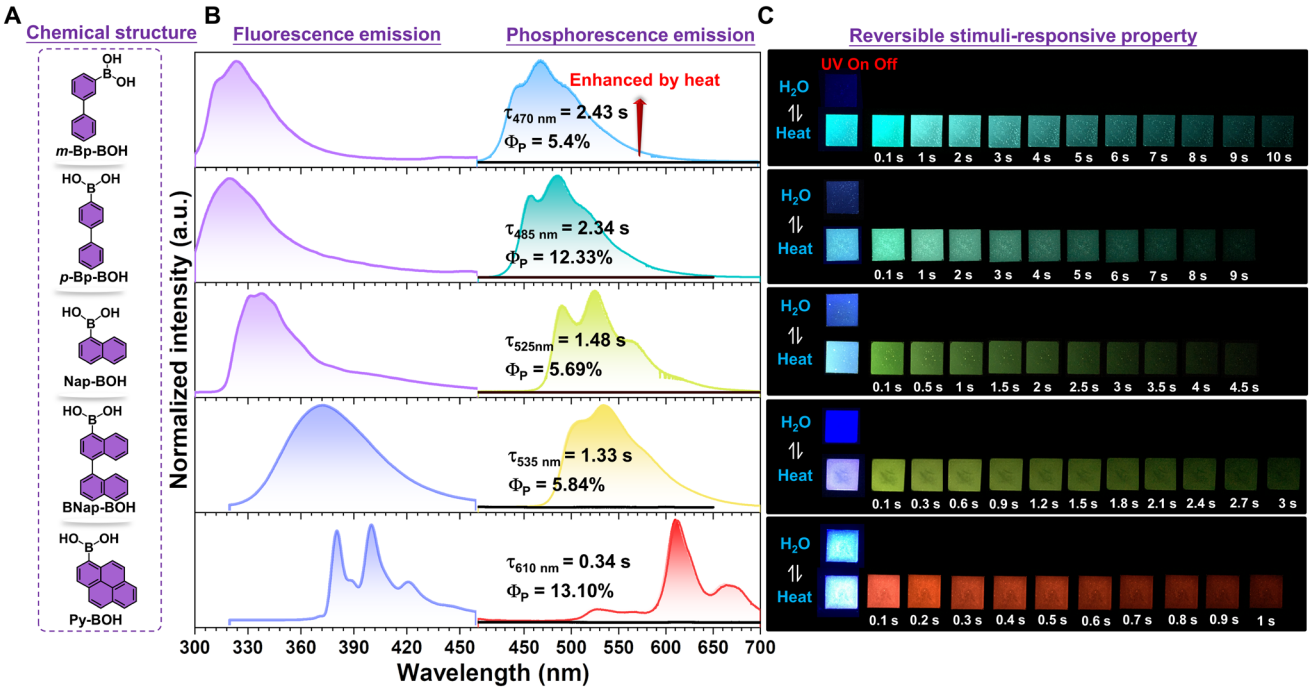

Fig. 2. Photophysical properties of five polymer films under the stimuli of water and heat. (**A**) Chemical structures of five arylboronic acids. (**B**) The steady-state photoluminescence spectra and phosphorescence spectra upon water fumigation or heating of *m*-Bp-BOH-PVA (λ_{ex} = 254 nm), *p*-Bp-BOH-PVA (λ_{ex} = 254 nm), Nap-BOH-PVA (λ_{ex} = 312 nm), BNap-BOH-PVA (λ_{ex} = 312 nm), and Py-BOH-PVA (λ_{ex} = 365 nm) films. Inset: Phosphoresce lifetimes and phosphoresce quantum yields of five polymer films after heating at 85°C for 10 min and dropping to room temperature. a.u., arbitrary units. (**C**) Photographs of the reversible heating/water fumigation processes for five polymer films.

The mechanism for stimulus-responsive RTP with color tunability

To explore the mechanism for RTP effect of these films, we prepared another five polymer films, namely, *m*-Bp-BOH-PVA-C, *p*-Bp-BOH-PVA-C, Nap-BOH-PVA-C, BNap-BOH-PVA-C, and Py-BOH-PVA-C, as a control. The only difference is that there was no addition of alkali to catalyze the reaction between arylboronic acid and PVA. Just as expected, the RTP performances of the control films are superior to arylboronic acid powder but inferior to the polymer films added alkali in terms of RTP emission intensity and lifetime even after heating (figs. S23 to S27). As shown in Fig. 3A, it could be found that when alkali was added to the catalyze reaction, the UV-vis absorption spectra of the obtained films would redshift compared with those without alkali. The change of the UV-vis absorption spectra may be derived from the formation of the B—O covalent bond between arylboronic acid and PVA. Because of the presence of the B—O covalent bond, the thermal motion of phosphorescent chromophores could be further restricted. By contrast, there were only intermolecular hydrogen bonding interactions but lack of similar B—O covalent bond in those control films, and their RTP performance was much inferior to that of films with B—O covalent bond. These findings of the research led to the conclusion that the ultralong RTP property is largely related to the formation of B—O covalent bond between arylboronic acids and PVA, which could enhance more effectively the rigidity of polymer matrix for generating long-lived phosphorescence emission under ambient condition. Furthermore, the phosphorescence spectra of five arylboronic acids in the solution state at 77 K are almost consistent with the RTP spectra of these films, suggesting that the phosphorescence emission source of films is from arylboronic acids (figs. S28 to S32).

To further investigate the water-sensitive mechanism of these films, we performed the Fourier transform infrared spectra. As illustrated in Fig. 3B, taking *m*-Bp-BOH-PVA film as an example, whether by heating or water fumigation, the film exhibits a noticeable peak at about 3300 cm^{-1}, which should be ascribed to the associated water and hydroxyl group of the adjacent *m*-Bp-BOH-PVA. Notably, after fumigation with water, the intensity of the peak at 3300 cm^{-1} becomes notable stronger, and the peak shape becomes wider compared with those of films after heating, proving that the water content in the film does increase and the presence of water could increase the degree of association with hydroxyl groups. Combined with changes in phosphorescence properties, it is considered that the presence of water destroys the hydrogen bonding interaction between adjacent *m*-Bp-BOH-PVA chains, leading to the destruction of the rigid environment of this system, and thus, no RTP emission was detected at this time. On the contrary, water was removed, and intermolecular hydrogen bonds were constructed again after heating the film, recovering the RTP property. Moreover, five control films without B—O covalent bond between PVA and arylboronic acids also showed the water-sensitive property (fig. S33). To sum up, it is revealed that the water-sensitive property of the *m*-Bp-BOH-PVA film should be related to the destruction and reconstruction of intermolecular hydrogen bond interaction between adjacent *m*-Bp-BOH-PVA chains, while the outstanding RTP performance mainly depends on the formation of the B—O covalent bond between PVA and arylboronic acid (fig. S34).

To further confirm that the degree of π conjugation from *m*-Bp-BOH-PVA to Py-BOH-PVA has increased, theoretical calculations were carried out (*41*). From the evaluated natural transition orbitals of five arylboronic acids shown in Fig. 3C, it could be concluded

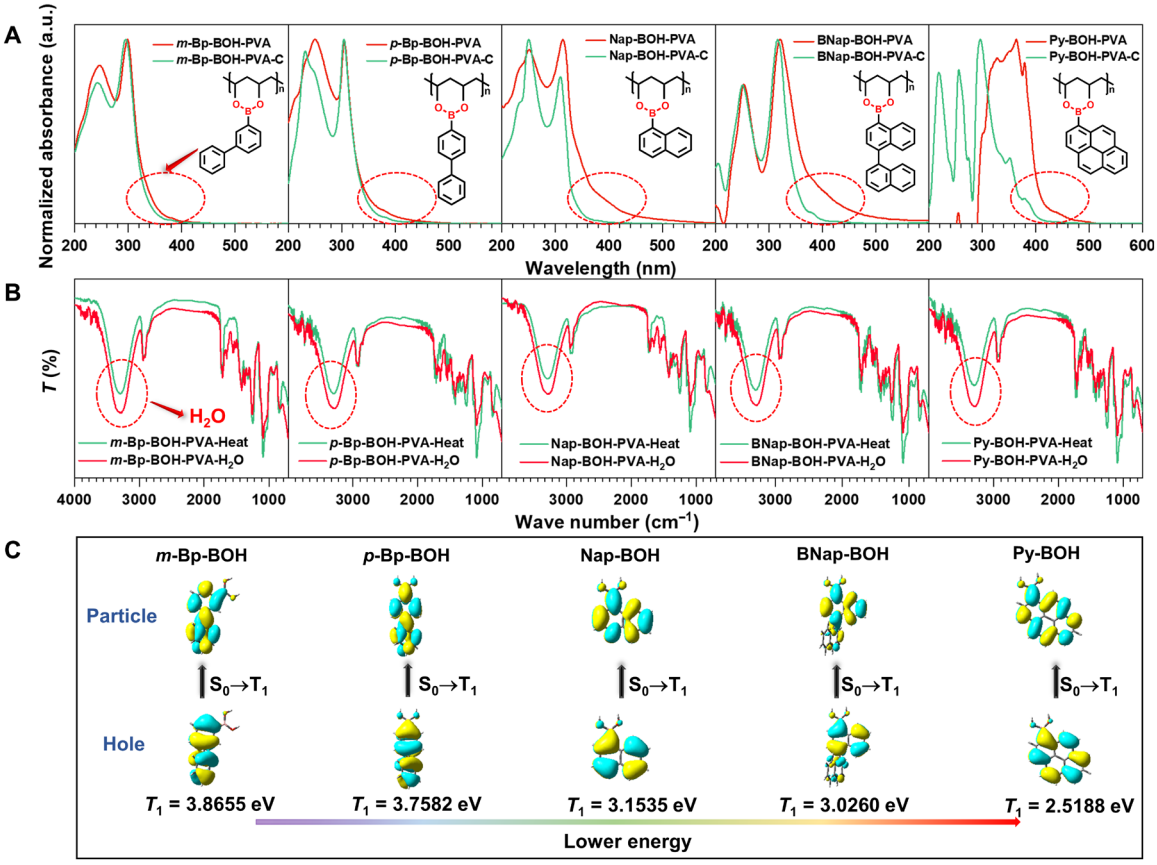

Fig. 3. The mechanism for stimulus-responsive room temperature phosphorescence with color tunability of five polymer films. (**A**) The absorption spectra of five polymer films and five corresponding control films and the chemical structures of *m*-Bp-BOH-PVA, *p*-Bp-BOH-PVA, Nap-BOH-PVA, BNap-BOH-PVA, and Py-BOH-PVA. (**B**) The Fourier transform infrared spectra of five polymer films under the heating/water stimuli. (**C**) The theoretical calculations about natural transition orbitals of T_1 states for *m*-Bp-BOH, *p*-Bp-BOH, Nap-BOH, BNap-BOH, and Py-BOH.

that the energy of T_1 decreases gradually with the extended degree of π conjugation, which is consistent with their experimental phenomena of the redshifted RTP emission. Moreover, as the energy gap between T_1 to S_0 becomes smaller for these phosphorescence chromophores, the nonradiative transition of triplet excitons would increase, leading to the shorted RTP lifetime (table S2).

Excitation wavelength–dependent RTP emission with stimulus-responsive property

To expand the practical application value of this system, we prepared a multicomponent excitation-dependent RTP film, namely, BNP-BOH-PVA. Combining the excitation spectra (figs. S35 to S39), time-resolved emission decay curves, and RTP quantum yields, *m*-Bp-BOH, Nap-BOH, and Py-BOH were chosen to react with PVA at a mass ratio of 1:1:5:500 (Fig. 4A). As expected, the RTP emission bands of the film showed a dynamically bathochromic shift from 470 to 610 nm with the excitation wavelength varying from 250 to 365 nm. As shown in Fig. 4B, the RTP emission was dominated by the blue-green luminescence when the excitation wavelength ranged from 250 to 280 nm, because *m*-Bp-BOH and Nap-BOH were mainly excited at this time. Certainly, the afterglow of the film was also visible to the naked eyes for about 7 s (fig. S40). When changing the excitation wavelength to 312 nm, the RTP emission band exhibited a significant redshift, mainly located at 530 nm. By this time, Py-BOH started to be excited, and the RTP emission of *m*-Bp-BOH became weaker. When the excitation wavelength was in the range of 340 to 365 nm, only Py-BOH was excited, and red long-lived luminescence was more intense. Meanwhile, the film is also sensitive to water, and the cycle by heating and water fumigation could also be repeated for many times (figs. S41 to S46). As a result, an amorphous stimulus-responsive RTP material with full-color tunability was developed successfully and conveniently, which is conducive to expand their practical applications in many fields (fig. S9).

Applications of stimulus-responsive RTP materials

Note that polymers are more attractive on account of their film-forming ability compared with organic small molecules, which is conducive to diverse technical applications with flexibility and easy processing procedures. In addition, completely aqueous processability is safer and nontoxic, and it could be used on substrates as an ink. It would not corrode or damage the substrate like organic solvents, which increases their practical application value.

Taking advantage of the different optimum excitation wavelengths and stimulus-responsive properties of *m*-Bp-BOH-PVA and Py-BOH-PVA, a multilevel information encryption was developed. As shown in Fig. 4F, the aqueous solution of mixed *m*-Bp-BOH-PVA and Py-BOH-PVA was used as ink to mark with "▬" and "•" on printing paper, respectively. When fumigated with water, no information

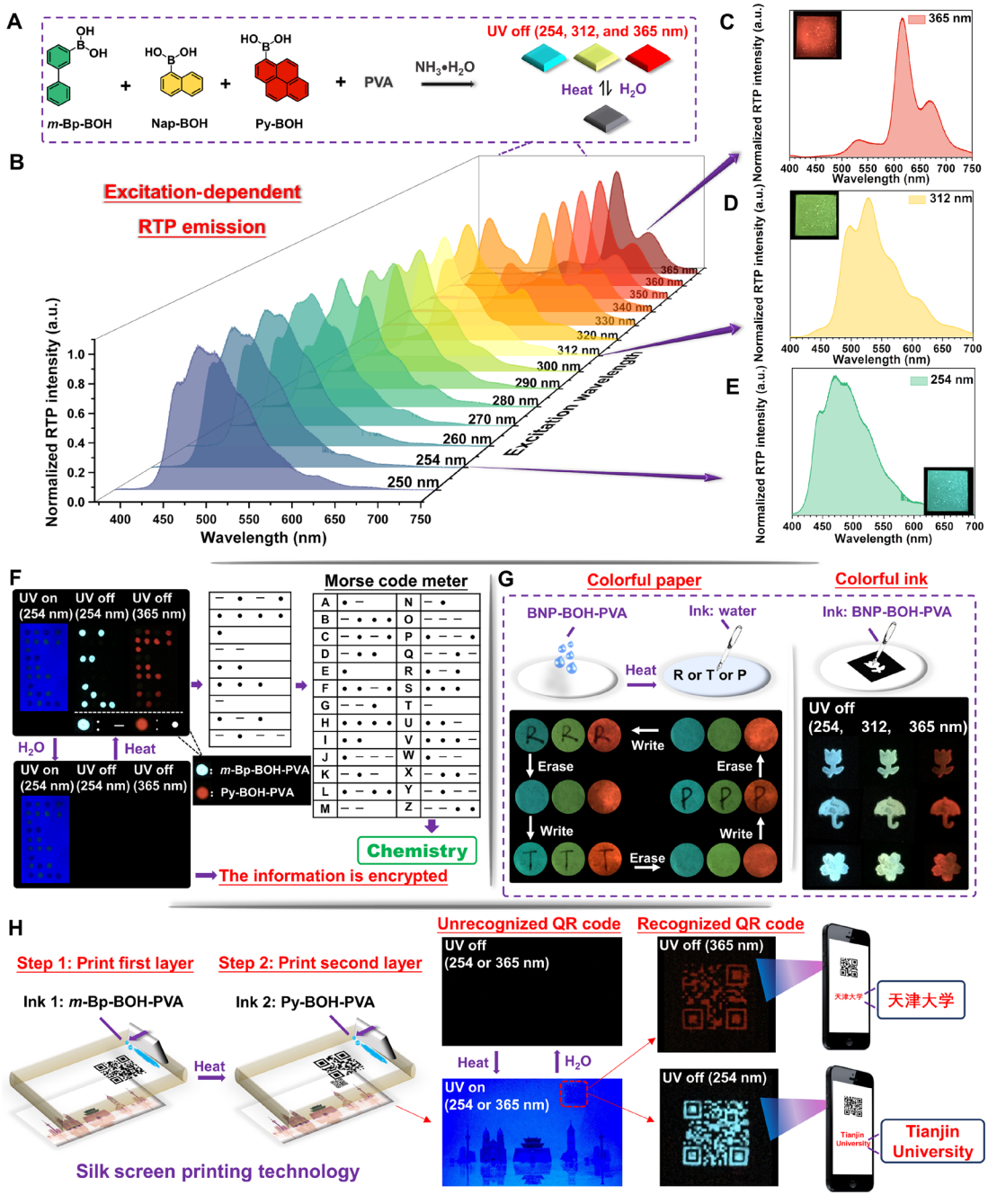

Fig. 4. Excitation wavelength–dependent RTP emission with stimulus-responsive property and corresponding applications. (**A**) Schematic illustration of the synthetic process of BNP-BOH-PVA film and changes with different excitation wavelengths under heating or water stimulus. (**B**) Phosphorescence spectra of the desiccative BNP-BOH-PVA film at different excitation wavelengths. Phosphorescence spectra of the desiccative BNP-BOH-PVA film when the excitation wavelengths are (**C**) 254, (**D**) 312, and (**E**) 365 nm. Inset: The corresponding photographs of the desiccative BNP-BOH-PVA film at different excitation wavelengths when the UV lamp was turned off. The schematic illustration of application process for (**F**) information encryption with Morse code, (**G**) multicolor paper and ink, and (**H**) information encryption with silk screen printing.

could be seen after turning off the UV lamp, and the information is encrypted, since the RTP emission of *m*-Bp-BOH-PVA and Py-BOH-PVA is inactive. Then, heating the paper until the water is removed. The information — is displayed after turning off the UV lamp with the wavelength of 254 nm, because only the RTP emission of *m*-Bp-BOH-PVA could be excited at this time, while the information • appears when the photoexcitation at 365 nm is stopped, because only the RTP emission of Py-BOH-PVA could be excited. According to the corresponding location of the information on the paper, the integrated Morse code could be obtained. Then, the comparison with the Morse code meter could get the final hidden information "chemistry." Morse code is an internationally unified cipher, and the

modification by excitation-dependent stimulus-response RTP materials could enhance the strength of the password, making it more confidential and international.

In addition, given the excitation dependence of BNP-BOH-PVA, a multicolor paper and multicolor ink were successfully prepared, respectively. As shown in Fig. 4G, the filter paper was soaked in the BNP-BOH-PVA aqueous solution, and then a piece of multicolor paper was obtained after drying. When excited by UV lamp with wavelengths of 254, 312, and 365 nm, respectively, three different colors of blue, yellow-green, and red were displayed after the UV lamp was turned off. Because the RTP emission could be quenched by water, the letter "R" was written on the paper with water. When UV irradiation was stopped, the nonemissive letter R was in sharp contrast to the afterglow of the paper where unquenched. Then, the letters would be erased after heating the paper. Thus, this kind of multicolor paper could be used for repeated writing by water and erasing by heating. On account of the excitation dependence of BNP-BOH-PVA, it also could be used to make multicolor ink. As shown in Fig. 4G, after being excited by UV irradiation with different wavelengths, the afterglow of the pattern showed different colors. Similarly, after fumigation with water, no patterns could be seen after turning off the UV lamp.

Last, another multilevel information encryption application using silk screen printing technology was explored. As shown in Fig. 4H, two quick response (QR) codes with different encryption information were printed in the same position one after another by using *m*-Bp-BOH-PVA and Py-BOH-PVA aqueous solutions as encryption inks, respectively. There is no valid information on paper upon the UV irradiation, no matter whether heated or not, because two QR codes are stacked together and the fluorescence of QR code cannot be recognized with the disguise of background fluorescence from the paper. However, after heating, when switching off the UV lamp with the wavelength of 254 nm, the QR code printed by *m*-Bp-BOH-PVA with blue afterglow was observed by the naked eyes under ambient condition. The encrypted information "天津大学" could be identified by cellphone, while the red afterglow of the QR code printed by Py-BOH-PVA could be observed by the naked eyes and another encrypted information "Tianjin University" could be identified by cellphone after stopping the UV irradiation with a wavelength of 365 nm. As a result, such a three-level information encryption was realized.

DISCUSSION

In summary, a new kind of stimulus-responsive ultralong RTP materials with full-color tunability was designed and prepared. The fabricated films after drying show the remarkable RTP property. Then, the RTP property of films disappears when exposed to a humid environment, because the water could break the rigid environment of the system. Conversely, the RTP performances of films are recovered after heating. Moreover, the BNP-BOH-PVA film exhibits excitation-dependent RTP property, which adjusts afterglow colors from blue to green, then to red as the excitation wavelength increases. Last, because of the water/heat-sensitive, excitation-dependent, and pure aqueous–processable properties of these films, they show promising applications in multilevel information encryption and multicolor paper and ink. The development of the stimulus-responsive color-tunable materials with ultralong afterglow will broaden multifunctional stimuli-responsive materials and expand applications in much more fields.

MATERIALS AND METHODS

Reagents and materials

Unless otherwise noted, all reagents used in the experiments were purchased from commercial sources. The PVA was purchased from Macklin ($M_W \approx 20000$, alcoholysis degree: 87 to 89%). 3-Biphenylboronic acid (purity: 98.75%) was purchased from Bide Pharmatech. 4-(1-Naphthyl)naphthalene-1-boronic acid (purity: 98%) was purchased from Aladdin. 4-Biphenylboronic acid (purity: 99%), 1-naphthylboronic acid (purity: 98%), and 1-pyrenylboronic acid (purity: 99%) were purchased from Heowns.

Measurements

UV-vis absorption spectra were obtained using a Shimadzu UV-2700. Steady-state photoluminescence/phosphorescence spectra and phosphorescence lifetime were measured using Hitachi F-4700. The fluorescence lifetime and photoluminescence quantum yield were obtained on FLS-1000. The luminescent photos were taken by iPhone 6s under the irradiation of handheld UV lamp at room temperature. The thermogravimetric analysis data were obtained on TG 209 F3. The differential scanning calorimetry (DSC) data were obtained on DSC 214 polyma. The powder x-ray diffraction patterns were obtained on MiniFlex600.

General procedure for synthesis of hybrids

m-Bp-BOH-PVA film

To a stirred solution of PVA (500 mg) in water (3 ml), 3-biphenylboronic acid (5 mg) in water (4 ml) and ammonium hydroxide (1 ml) were added. A stock solution of 3-biphenylboronic acid (3.16 mmol/liter; 0.625 mg/ml) and PVA (1.42 mol/liter; 62.5 mg/ml) was obtained. The mixture was stirred at 80°C for 20 min. Subsequently, 0.7 ml of the obtained aqueous solution was taken and dropped on the cover glass with a syringe. Then, the cover glass was heated until the water evaporates to obtain a film with thickness of about 15 μm.

p-Bp-BOH-PVA film

To a stirred solution of PVA (500 mg) in water (3 ml), 4-biphenylboronic acid (5 mg) in water (4 ml) and ammonium hydroxide (1 ml) were added. A stock solution of 4-biphenylboronic acid (3.16 mmol/liter; 0.625 mg/ml) and PVA (1.42 mol/liter; 62.5 mg/ml) was obtained. The mixture was stirred at 80°C for 20 min. Subsequently, 0.7 ml of the obtained aqueous solution was taken and dropped on the cover glass with a syringe. Then, the cover glass was heated until the water evaporates.

Nap-BOH-PVA film

To a stirred solution of PVA (500 mg) in water (3 ml), 1-naphthylboronic acid (5 mg) in water (4 ml) and ammonium hydroxide (1 ml) were added. A stock solution of 1-naphthylboronic acid (3.63 mmol/liter; 0.625 mg/ml) and PVA (1.42 mol/liter; 62.5 mg/ml) was obtained. The mixture was stirred at 80°C for 20 min. Subsequently, 0.7 ml of the obtained aqueous solution was taken and dropped on the cover glass with a syringe. Then, the cover glass was heated until the water evaporates.

BNap-BOH-PVA film

To a stirred solution of PVA (500 mg) in water (3 ml), 4-(1-naphthyl) naphthalene-1-boronic acid (5 mg) in water (4 ml) and ammonium hydroxide (1 ml) were added. A stock solution of 4-(1-naphthyl) naphthalene-1-boronic acid (2.10 mmol/liter; 0.625 mg/ml) and PVA (1.42 mol/liter; 62.5 mg/ml) was obtained. The mixture was stirred at 80°C for 20 min. Subsequently, 0.7 ml of the obtained aqueous solution was taken and dropped on the cover glass with a syringe. Then, the cover glass was heated until the water evaporates.

Py-BOH-PVA film

To a stirred solution of PVA (500 mg) in water (3 ml), 1-pyrenylboronic acid (10 mg) in water (4 ml) and ammonium hydroxide (1 ml) were added. A stock solution of 1-pyrenylboronic acid (5.04 mmol/liter; 1.25 mg/ml) and PVA (1.42 mol/liter; 62.5 mg/ml) was obtained. The mixture was stirred at 80°C for 20 min. Subsequently, 0.7 ml of the obtained aqueous solution was taken and dropped on the cover glass with a syringe. Then, the cover glass was heated until the water evaporates.

m-Bp-BOH-PVA-C film

To a stirred solution of PVA (500 mg) in water (3 ml), 3-biphenylboronic acid (5 mg) in water (5 ml) was added. A stock solution of 3-biphenylboronic acid (3.16 mmol/liter; 0.625 mg/ml) and PVA (1.42 mol/liter; 62.5 mg/ml) was obtained. The mixture was stirred at 80°C for 20 min. Subsequently, 0.7 ml of the obtained aqueous solution was taken and dropped on the cover glass with a syringe. Then, the cover glass was heated until the water evaporates.

p-Bp-BOH-PVA-C film

To a stirred solution of PVA (500 mg) in water (3 ml), 4-biphenylboronic acid (5 mg) in water (5 ml) was added. A stock solution of 4-biphenylboronic acid (3.16 mmol/liter; 0.625 mg/ml) and PVA (1.42 mol/liter; 62.5 mg/ml) was obtained. The mixture was stirred at 80°C for 20 min. Subsequently, 0.7 ml of the obtained aqueous solution was taken and dropped on the cover glass with a syringe. Then, the cover glass was heated until the water evaporates.

Nap-BOH-PVA-C film

To a stirred solution of PVA (500 mg) in water (3 ml), 1-naphthylboronic acid (5 mg) in water (5 ml) was added. A stock solution of 1-naphthylboronic acid (3.63 mmol/liter; 0.625 mg/ml) and PVA (1.42 mol/liter; 62.5 mg/ml) was obtained. The mixture was stirred at 80°C for 20 min. Subsequently, 0.7 ml of the obtained aqueous solution was taken and dropped on the cover glass with a syringe. Then, the cover glass was heated until the water evaporates.

BNap-BOH-PVA-C film

To a stirred solution of PVA (500 mg) in water (3 ml), 4-(1-naphthyl) naphthalene-1-boronic acid (5 mg) in water (5 ml) was added. A stock solution of 4-(1-naphthyl)naphthalene-1-boronic acid (2.10 mmol/liter; 0.625 mg/ml) and PVA (1.42 mol/liter; 62.5 mg/ml) was obtained. The mixture was stirred at 80°C for 20 min. Subsequently, 0.7 ml of the obtained aqueous solution was taken and dropped on the cover glass with a syringe. Then, the cover glass was heated until the water evaporates.

Py-BOH-PVA-C film

To a stirred solution of PVA (500 mg) in water (3 ml), 1-pyrenylboronic acid (10 mg) in water (5 ml) was added. A stock solution of 1-pyrenylboronic acid (5.04 mmol/liter; 1.25 mg/ml) and PVA (1.42 mol/liter; 62.5 mg/ml) was obtained. The mixture was stirred at 80°C for 20 min. Subsequently, 0.7 ml of the obtained aqueous solution was taken and dropped on the cover glass with a syringe. Then, the cover glass was heated until the water evaporates.

BNP-BOH-PVA film

To a stirred solution of PVA (500 mg) in water (3 ml), 3-biphenylboronic acid (1 mg), 1-naphthylboronic acid (1 mg), 1-pyrenylboronic acid (5 mg) in water (4 ml), and ammonium hydroxide (1 ml) were added. A stock solution of 3-biphenylboronic acid (0.63 mmol/liter; 0.125 mg/ml), 1-naphthylboronic acid (0.73 mmol/liter; 0.125 mg/liter), 1-pyrenylboronic acid (2.52 mmol/liter; 0.625 mg/ml), and PVA (1.42 mol/liter; 62.5 mg/ml) was obtained. The mixture was stirred at 80°C for 20 min. Subsequently, 0.7 ml of the obtained aqueous solution was taken and dropped on the cover glass with a syringe. Then, the cover glass was heated until the water evaporates.

Theoretical calculation

All density functional theory calculations were performed using the Gaussian 09 program. The ground state (S_0) structures and natural transition orbits of T_1 states for *m*-Bp-BOH, *p*-Bp-BOH, Nap-BOH, BNap-BOH, and Py-BOH were evaluated by the TD-m062x/6-31g*.

SUPPLEMENTARY MATERIALS

Supplementary material for this article is available at https://science.org/doi/10.1126/sciadv.abl8392

REFERENCES AND NOTES

1. S. Kim, S. Yoon, S. Y. Park, Highly fluorescent chameleon nanoparticles and polymer films: Multicomponent organic systems that combine FRET and photochromic switching. *J. Am. Chem. Soc.* **134**, 12091–12097 (2012).
2. X. Wang, H. Ma, M. Gu, C. Lin, N. Gan, Z. Xie, H. Wang, L. Bian, L. Fu, S. Cai, Z. Chi, W. Yao, Z. An, H. Shi, W. Huang, Multicolor ultralong organic phosphorescence through alkyl engineering for 4D coding applications. *Chem. Mater.* **31**, 5584–5591 (2019).
3. D. Kim, A. D'Aléo, X. Chen, A. D. S. Sandanayaka, D. Yao, L. Zhao, T. Komino, E. Zaborova, G. Canard, Y. Tsuchiya, E. Choi, J. W. Wu, F. Fages, J. Brédas, J. Ribierre, C. Adachi, High-efficiency electroluminescence and amplified spontaneous emission from a thermally activated delayed fluorescent near-infrared emitter. *Nat. Photonics* **12**, 98–104 (2018).
4. S. Jia, W. Fong, B. Graham, B. J. Boyd, Photoswitchable molecules in long-wavelength light-responsive drug delivery: From molecular design to applications. *Chem. Mater.* **30**, 2873–2887 (2018).
5. Z. Zhang, Y. Wu, K. Tang, C. Chen, J. Ho, J. Su, H. Tian, P. Chou, Excited-state conformational/electronic responses of saddle-shaped *N,N'*-disubstituted-dihydrodibenzo[*a,c*]phenazines: Wide-tuning emission from red to deep blue and white light combination. *J. Am. Chem. Soc.* **137**, 8509–8520 (2015).
6. S. Yagai, S. Okamura, Y. Nakano, M. Yamauchi, K. Kishikawa, T. Karatsu, A. Kitamura, A. Ueno, D. Kuzuhara, H. Yamada, T. Seki, H. Ito, Design amphiphilic dipolar π-systems for stimuli-responsive luminescent materials using metastable states. *Nat. Commun.* **5**, 4013 (2014).
7. Y. Xie, Z. Li, Triboluminescence: Recalling interest and new aspects. *Chem* **4**, 943–971 (2018).
8. D. Wang, T. Imae, Fluorescence emission from dendrimers and its pH dependence. *J. Am. Chem. Soc.* **126**, 13204–13205 (2004).
9. J. Mei, N. L. C. Leung, R. T. K. Kwok, J. W. Y. Lam, B. Z. Tang, Aggregation-induced emission: Together we shine, united we soar. *Chem. Rev.* **115**, 11718–11940 (2015).
10. Z. Gao, Y. Han, F. Wang, Cooperative supramolecular polymers with anthracene-endoperoxide photo-switching for fluorescent anti-counterfeiting. *Nat. Commun.* **9**, 3977 (2018).
11. Y. Matsunaga, J. Yang, Multicolor fluorescence writing based on host–guest interactions and force-induced fluorescence-color memory. *Angew. Chem. Int. Ed.* **54**, 7985–7989 (2015).
12. E. Y. Zhou, H. J. Knox, C. Liu, W. Zhao, J. Chan, A conformationally restricted aza-BODIPY platform for stimulus-responsive probes with enhanced photoacoustic properties. *J. Am. Chem. Soc.* **141**, 17601–17609 (2019).
13. H. S. Afsari, M. C. D. Santos, S. Lindén, T. Chen, X. Qiu, P. Henegouwen, T. Jennings, K. Susumu, I. Medintz, N. Hildebrandt, L. Miller, Time-gated FRET nanoassemblies for rapid and sensitive intra- and extracellular fluorescence imaging. *Sci. Adv.* **2**, e1600265 (2016).
14. Z. Chen, P. Yan, L. Zou, M. Zhao, J. Jiang, S. Liu, K. Y. Zhang, W. Huang, Q. Zhao, Using ultrafast responsive phosphorescent nanoprobe to visualize elevated peroxynitrite in vitro and in vivo via ratiometric and time-resolved photoluminescence imaging. *Adv. Healthc. Mater.* **7**, e1800309 (2018).
15. Q. Wu, K. Y. Zhang, P. Dai, H. Zhu, Y. Wang, L. Song, L. Wang, S. Liu, Q. Zhao, W. Huang, Bioorthogonal "labeling after recognition" affording an FRET-based luminescent probe for detecting and imaging caspase-3 via photoluminescence lifetime imaging. *J. Am. Chem. Soc.* **142**, 1057–1064 (2020).
16. J. Yang, M. Fang, Z. Li, Stimulus-responsive room temperature phosphorescence in purely organic luminogens. *InfoMat.* **2**, 791–806 (2020).
17. L. Huang, C. Qian, Z. Ma, Stimuli-responsive purely organic room-temperature phosphorescence materials. *Chem. A Eur. J.* **26**, 11914–11930 (2020).
18. F. Yu, W. Liu, B. Li, D. Tian, J. Zuo, Q. Zhang, Photostimulus-responsive large-area two-dimensional covalent organic framework films. *Angew. Chem. Int. Ed.* **58**, 16101–16104 (2019).

19. Y. Gong, G. Chen, Q. Peng, W. Z. Yuan, Y. Xie, S. Li, Y. Zhang, B. Z. Tang, Achieving persistent room temperature phosphorescence and remarkable mechanochromism from pure organic luminogens. *Adv. Mater.* **27**, 6195–6201 (2015).
20. J. Yang, M. Fang, Z. Li, Stimulus-responsive room temperature phosphorescence materials: Internal mechanism, design strategy, and potential application. *Acc. Mater. Res.* **2**, 644–654 (2021).
21. Z. Wang, Y. Zhang, C. Wang, X. Zheng, Y. Zheng, L. Gao, C. Yang, Y. Li, L. Qu, Y. Zhao, Color-tunable polymeric long-persistent luminescence based on polyphosphazenes. *Adv. Mater.* **32**, 1907355 (2020).
22. L. Ma, S. Sun, B. Ding, X. Ma, H. Tian, Highly efficient room-temperature phosphorescence based on single-benzene structure molecules and photoactivated luminescence with afterglow. *Adv. Funct. Mater.* **31**, 2010659 (2021).
23. Y. Zhang, L. Gao, X. Zheng, Z. Wang, C. Yang, H. Tang, L. Qu, Y. Li, Y. Zhao, Ultraviolet irradiation-responsive dynamic ultralong organic phosphorescence in polymeric systems. *Nat. Commun.* **12**, 2297 (2021).
24. S. Hirata, K. Totani, J. Zhang, T. Yamashita, H. Kaji, S. R. Marder, T. Watanabe, C. Adachi, Efficient persistent room temperature phosphorescence in organic amorphous materials under ambient conditions. *Adv. Funct. Mater.* **23**, 3386–3397 (2013).
25. X. Ma, J. Wang, H. Tian, Assembling-induced emission: An efficient approach for amorphous metal-free organic emitting materials with room-temperature phosphorescence. *Acc. Chem. Res.* **52**, 738–748 (2019).
26. X. Ma, C. Xu, J. Wang, H. Tian, Amorphous pure organic polymers for heavy-atom-free efficient room-temperature phosphorescence emission. *Angew. Chem. Int. Ed.* **57**, 10854–10858 (2018).
27. Y. Su, S. Z. F. Phua, Y. Li, X. Zhou, D. Jana, G. Liu, W. Q. Lim, W. K. Ong, C. Yang, Y. Zhao, Ultralong room temperature phosphorescence from amorphous organic materials toward confidential information encryption and decryption. *Sci. Adv.* **4**, eaas9732 (2018).
28. D. Lee, O. Bolton, B. C. Kim, J. H. Youk, S. Takayama, J. Kim, Room temperature phosphorescence of metal-free organic materials in amorphous polymer matrices. *J. Am. Chem. Soc.* **135**, 6325–6329 (2013).
29. N. Gan, H. Shi, Z. An, W. Huang, Recent advances in polymer-based metal-free room-temperature phosphorescent materials. *Adv. Funct. Mater.* **28**, 1802657 (2018).
30. Y. Su, Y. Zhang, Z. Wang, W. Gao, P. Jia, D. Zhang, C. Yang, Y. Li, Y. Zhao, Excitation-dependent long-life luminescent polymeric systems under ambient conditions. *Angew. Chem. Int. Ed.* **59**, 9967–9971 (2020).
31. J. Wang, Y. Fang, C. Li, L. Niu, W. Fang, G. Cui, Q. Yang, Time-dependent afterglow color in a single-component organic molecular crystal. *Angew. Chem. Int. Ed.* **59**, 10032–10036 (2020).
32. L. Gu, H. Shi, L. Bian, M. Gu, K. Ling, X. Wang, H. Ma, S. Cai, W. Ning, L. Fu, H. Wang, S. Wang, Y. Gao, W. Yao, F. Huo, Y. Tao, Z. An, X. Liu, W. Huang, Colour-tunable ultra-long organic phosphorescence of a single-component molecular crystal. *Nat. Photonics* **13**, 406–411 (2019).
33. J. Chen, T. Yu, E. Ubba, Z. Xie, Z. Yang, Y. Zhang, S. Liu, J. Xu, M. P. Aldred, Z. Chi, Achieving dual-emissive and time-dependent evolutive organic afterglow by bridging molecules with weak intermolecular hydrogen bonding. *Adv. Opt. Mater.* **7**, 1801593 (2019).
34. L. Gu, H. Wu, H. Ma, W. Ye, W. Jia, H. Wang, H. Chen, N. Zhang, D. Wang, C. Qian, Z. An, W. Huang, Y. Zhao, Color-tunable ultralong organic room temperature phosphorescence from a multicomponent copolymer. *Nat. Commun.* **11**, 944 (2020).
35. X. Dou, T. Zhu, Z. Wang, W. Sun, Y. Lai, K. Sui, Y. Tan, Y. Zhang, W. Z. Yuan, Color-tunable, excitation-dependent, and time-dependent afterglows from pure organic amorphous polymers. *Adv. Mater.* **32**, 2004768 (2020).
36. J. Yang, Z. Ren, Z. Xie, Y. Liu, C. Wang, Y. Xie, Q. Peng, B. Xu, W. Tian, F. Zhang, Z. Chi, Q. Li, Z. Li, AIEgen with fluorescence-phosphorescence dual mechanoluminescence at room temperature. *Angew. Chem. Int. Ed.* **56**, 880–884 (2017).
37. R. Tian, S.-M. Xu, Q. Xu, C. Lu, Large-scale preparation for efficient polymer-based room-temperature phosphorescence via click chemistry. *Sci. Adv.* **6**, eaaz6107 (2020).
38. H. Zheng, P. Cao, Y. Wang, X. Lu, P. Wu, Ultralong room-temperature phosphorescence from boric acid. *Angew. Chem. Int. Ed.* **60**, 9500–9506 (2021).
39. H. Zheng, Y. Wang, P. Cao, P. Wu, Color-tunable ultralong room temperature phosphorescence from EDTA. *Chem. Commun.* **57**, 3575–3578 (2021).
40. B. Ding, L. Ma, Z. Huang, X. Ma, H. Tian, Engendering persistent organic room temperature phosphorescence by trace ingredient incorporation. *Sci. Adv.* **7**, eabf9668 (2021).
41. B. DeHaven, D. Goodlett, A. Sindt, N. Noll, M. Vetta, M. Smith, C. Martin, L. Gonzalez, L. Shimizu, Enhancing the stability of photogenerated benzophenone triplet radical pairs through supramolecular assembly. *J. Am. Chem. Soc.* **140**, 13064–13070 (2018).

Acknowledgments

Funding: We are grateful to the National Natural Science Foundation of China (no. 51903188), the Natural Science Foundation of Tianjin City (no. 19JCQNJC04500), the Open Project Program of Wuhan National Laboratory for Optoelectronics (no. 2020WNLOKF013), the starting grants of Tianjin University and Tianjin Government, and Independent Innovation Fund of Tianjin University for financial support. **Author contributions:** Conceptualization: J.Y. and Z.L. Methodology: Z.L. and J.Y. Investigation: D.L. and J.Y. Visualization: D.L. and M.F. Funding acquisition: Z.L. and J.Y. Project administration: Z.L. and J.Y. Supervision: J.Y., B.Z.T., and Z.L. Writing (original draft): D.L. Writing (review and editing): J.Y. and Z.L. **Competing interests:** D.L., J.Y., M.F., and Z.L. are co-inventors on two provisional patent applications related to this work filed at the China National Intellectual Property Administration (no. 202111068009.2, filed 13 September 2021; no. 202111068955.7, filed 13 September 2021). The authors declare that they have no other competing interests. **Data and materials availability:** All data needed to evaluate the conclusions in the paper are present in the paper and/or the Supplementary Materials.

Submitted 9 August 2021
Accepted 4 January 2022
Published 25 February 2022
10.1126/sciadv.abl8392